Supporting Information

Atomic insights into the electrocatalytic properties of La*B*O_3 perovskite oxides for lithium−sulfur batteries performance

Lirong Zhang[1], Qi Jin[1], Fengfeng Han[1], Zhiguo Zhang[2], Xitian Zhang[1,*], and Lili Wu[1,*]

1. *Key Laboratory for Photonic and Electronic Bandgap Materials, Ministry of Education, School of Physics and Electronic Engineering, Harbin Normal University, Harbin 150025, People's Republic of China.*
2. *Department of Physics, Harbin Institute of Technology, Harbin 150001, People's Republic of China.*

[*]Corresponding authors' emails: xtzhangzhang@hotmail.com (X.T. Zhang), wll790107@hotmail.com (L.L. Wu).

Note 1: Detailed information regarding the calculation of Gibbs free energy

The Gibbs free energy of the above reactions can be expressed as:

$$G(T) = E_{\mathrm{DFT}} + G^{corr}(T) = E_{\mathrm{DFT}} + ZPE + \Delta H_{0\to T} - TS_{vib}(T) \#(1)$$

Where E_{DFT} electron energy is calculated by VASP. $G^{corr}(T)$ is the thermodynamic correction related to the Gibbs free energy. *ZPE* represents the zero–point energy. $\Delta H_{0\to T}$ and $S_{vib}(T)$ represent the correction of enthalpy and entropy at the room temperature of 298 K, respectively. The calculated values of *ZPE*, $\Delta H_{0\to T}$, and S_{vib} are obtained through the VASPKIT code [1].

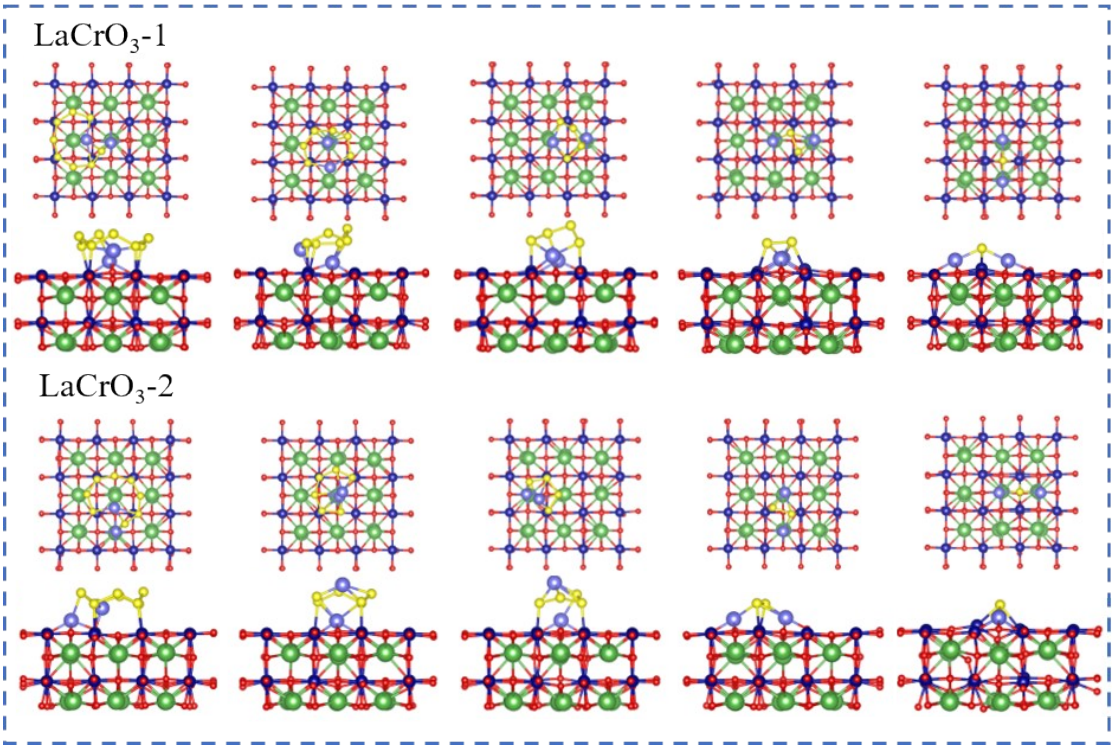

Figure S1. Two structural configurations of adsorbed Li_2S_n (n = 1, 2, 4, 6, and 8) on $LaCrO_3$ surface.

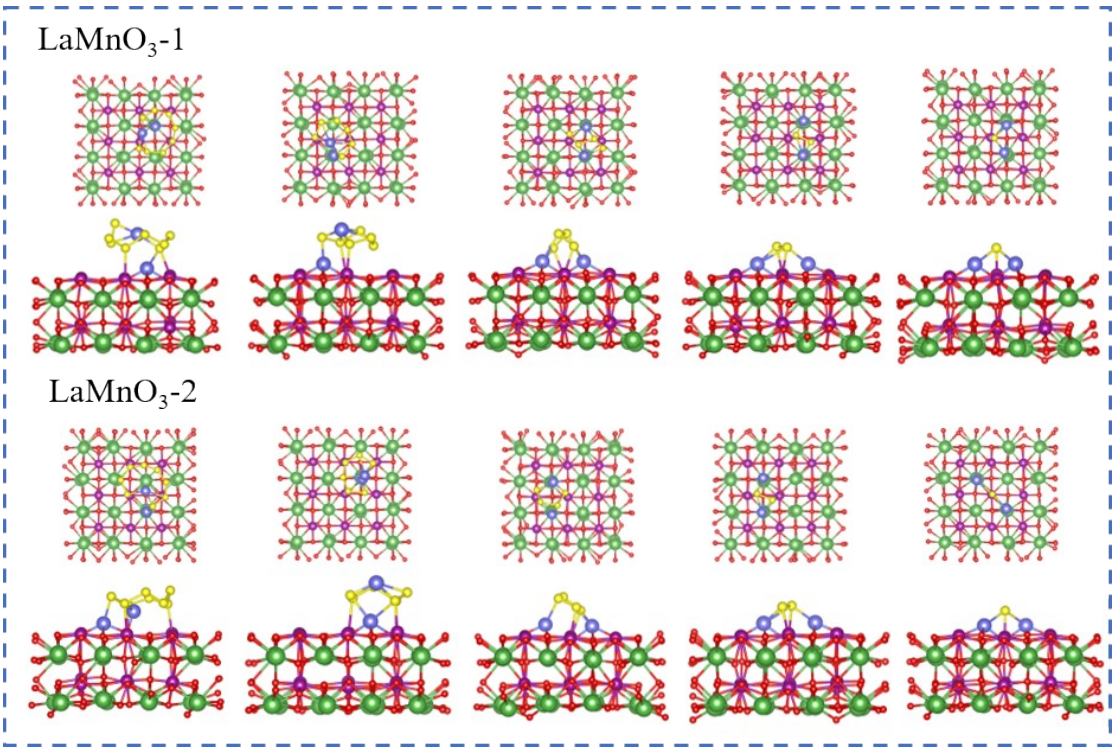

Figure S2. Two structural configurations of adsorbed Li_2S_n (n = 1, 2, 4, 6, and 8) on $LaMnO_3$ surface.

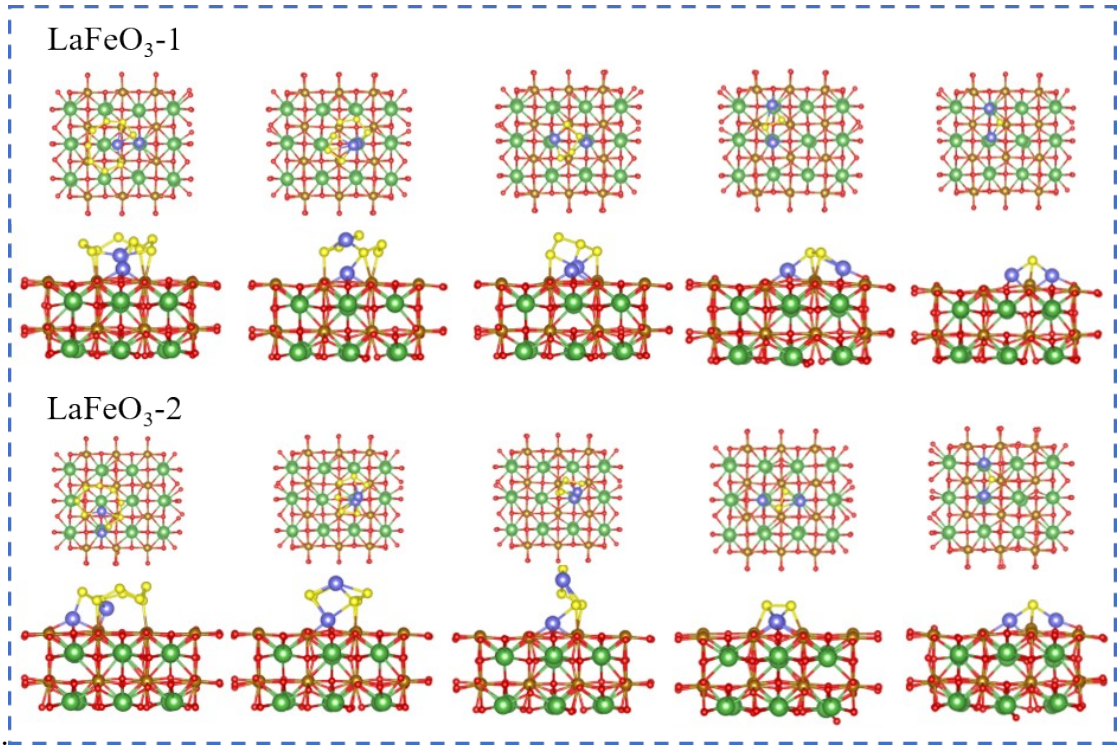

Figure S3. Two structural configurations of adsorbed Li_2S_n (n = 1, 2, 4, 6, and 8) on $LaFeO_3$ surface.

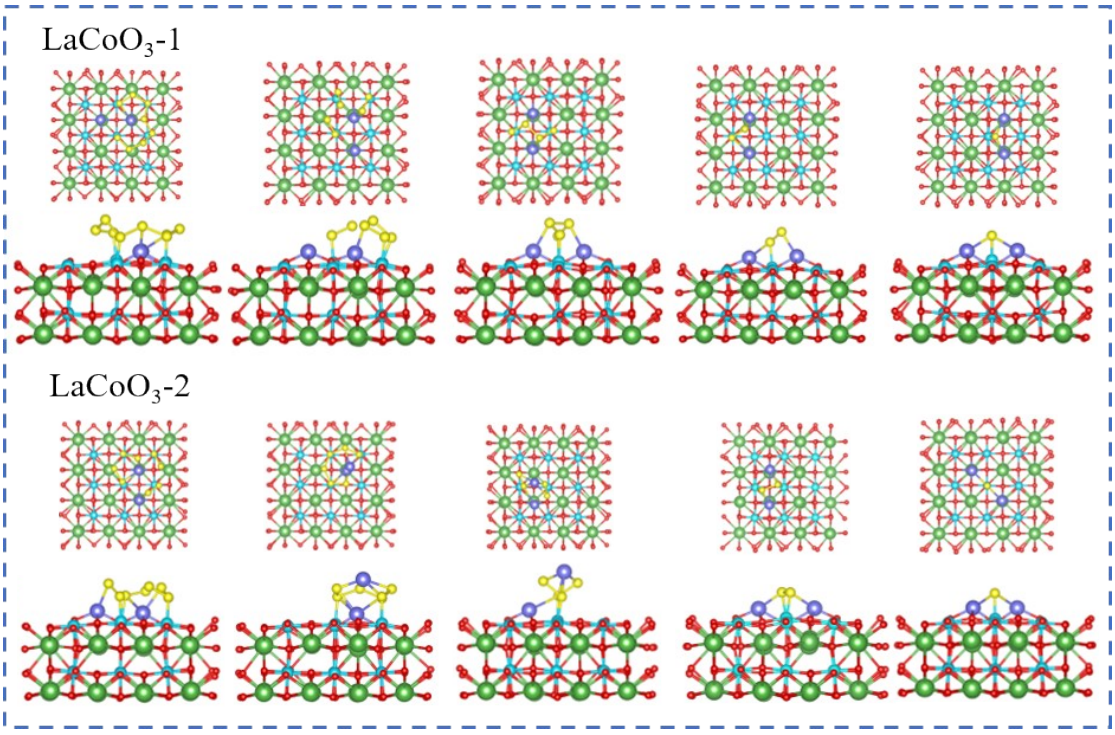

Figure S4. Two structural configurations of adsorbed Li_2S_n (n = 1, 2, 4, 6, and 8) on $LaCoO_3$ surface.

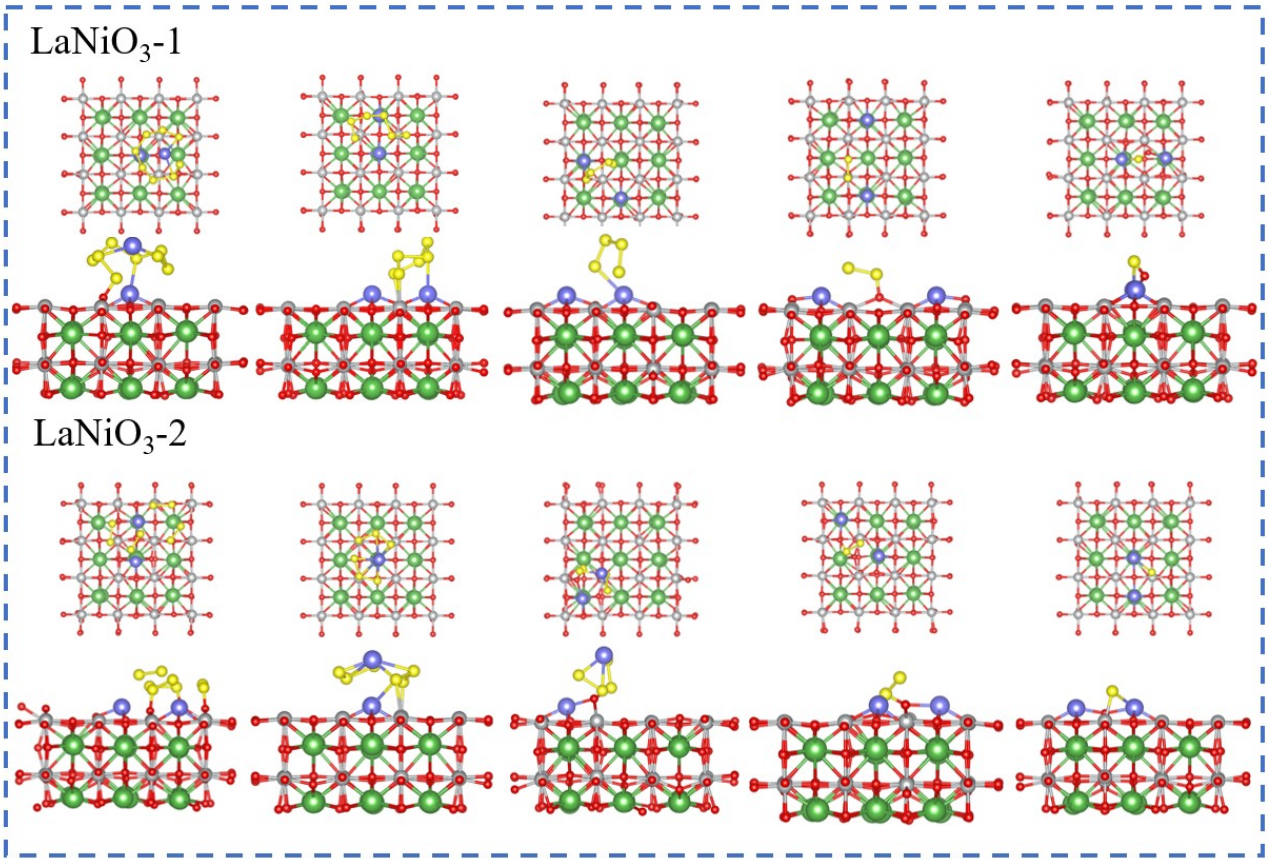

Figure S5. Two structural configurations of adsorbed Li_2S_n (n = 1, 2, 4, 6, and 8) on $LaNiO_3$ surface.

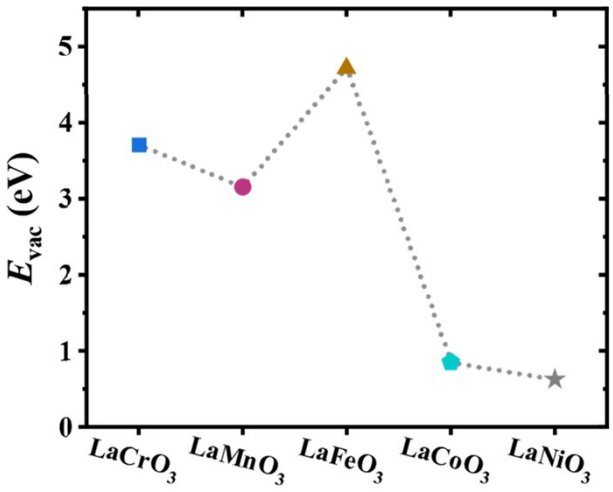

Figure S6. Oxygen vacancy formation energies of LaBO$_3$ (B = Cr, Mn, Fe, Co, and Ni).

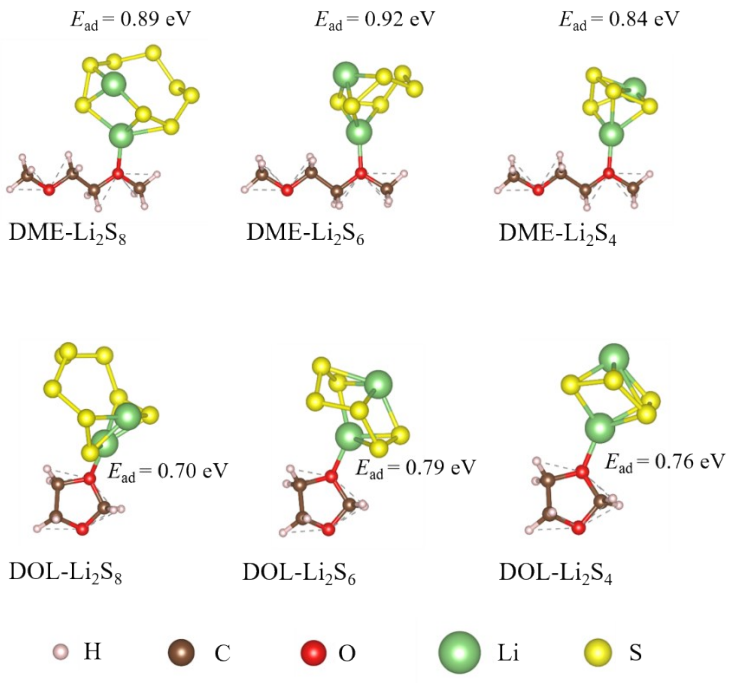

Figure S7. Structural configurations of soluble Li_2S_n in DOL/DME and corresponding adsorption energies.

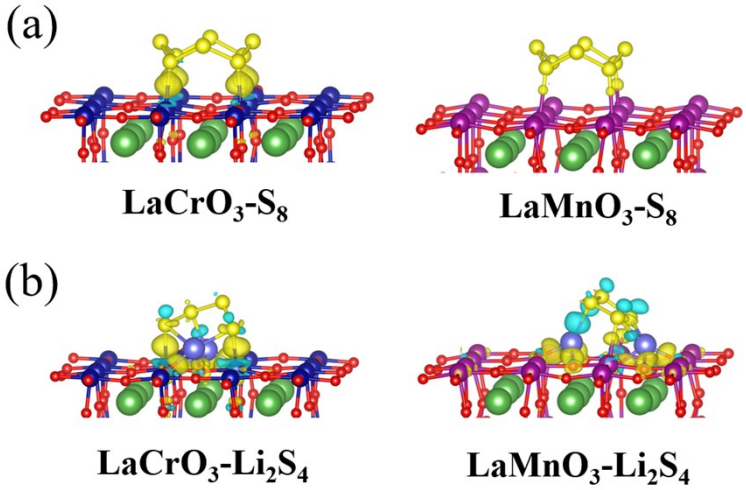

Figure S8. Difference charge density of (a) S_8 and (b) Li_2S_4 adsorbed on $LaCrO_3$ and $LaMnO_3$ with isosurface value of 0.004 e/Å^3.

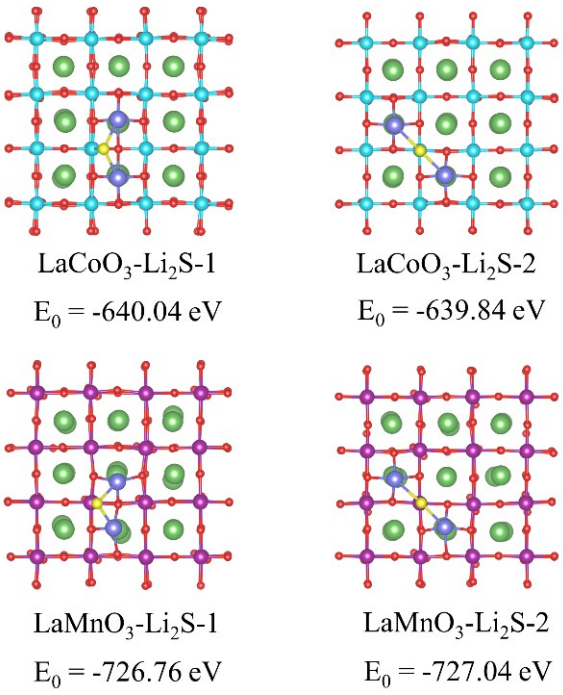

Figure S9. Two initial state structures of Li_2S decomposition on $LaMnO_3$ and $LaCoO_3$ surfaces.

We initially constructed two adsorption configurations for Li_2S and selected the most stable structure, characterized by the lowest energy as the starting point for the Li_2S decomposition study. As shown in Figure S8, $LaCoO_3$ serves as a representative example and is compared with $LaMnO_3$. It was found that the $LaCoO_3$-Li_2S-1 configuration exhibits lower energy and greater stability compared to the $LaCoO_3$-Li_2S-2 configuration, making it the chosen initial state for Li_2S decomposition. In contrast, the $LaMnO_3$-Li_2S-2 configuration is more stable. This difference in the initial state of Li_2S on $LaMnO_3$, compared to the other La*B*O_3 surfaces, leads to a distinct decomposition pathway for Li_2S.

Table S1. Computational and experimental lattice constants of LaBO$_3$ (B = Cr, Mn, Fe, Co, and Ni).

	$LaCrO_3$ (Å)	$LaMnO_3$ (Å)	$LaFeO_3$ (Å)	$LaCoO_3$ (Å)	$LaNiO_3$ (Å)
Computational	3.92	3.94	3.96	3.82	3.85
Experimental	3.89[2]	3.95[3]	3.93[4]	3.85[5]	3.85[4]

Table S2. Adsorption energies correspond to the two configurations of adsorbed Li_2S_n (n = 1, 2, 4, 6, and 8) on LaBO$_3$ (B = Cr, Mn, Fe, Co, and Ni) surfaces.

	$LaCrO_3$	$LaMnO_3$	$LaFeO_3$	$LaCoO_3$	$LaNiO_3$
E_{p1}-Li_2S_8 (eV)	4.99	4.64	3.61	8.54	5.55
E_{p2}-Li_2S_8 (eV)	4.97	5.44	3.58	8.21	9.89
E_{p1}-Li_2S_6 (eV)	4.40	4.54	3.24	7.67	5.48
E_{p2}-Li_2S_6 (eV)	3.58	4.23	2.86	5.59	3.13
E_{p1}-Li_2S_4 (eV)	4.18	4.99	3.51	7.42	5.62
E_{p2}-Li_2S_4 (eV)	3.24	5.20	2.11	4.52	4.13
E_{p1}-Li_2S_2 (eV)	4.58	5.67	2.96	6.89	9.63
E_{p2}-Li_2S_2 (eV)	4.50	5.66	4.02	7.26	7.13
E_{p1}-Li_2S (eV)	4.65	5.53	4.27	6.87	6.21
E_{p2}-Li_2S (eV)	4.65	5.79	4.48	6.66	8.06

Table S3. Calculated values of R_{vdW}, E_{ad}^{vdW}, and E_{ad}^{no-vdW} based on the adsorption configurations of S_8/Li_2S_n (n = 1, 2, 4, 6, and 8) on LaBO$_3$ (B = Cr, Mn, Fe, Co, and Ni) surfaces.

	$LaCrO_3$	$LaMnO_3$	$LaFeO_3$	$LaCoO_3$	$LaNiO_3$
E_{ad}^{vdW}-S_8 (eV)	-2.13	-2.91	-1.40	-3.11	-1.86
E_{ad}^{no-vdW}-S_8 (eV)	-0.73	-1.74	-0.29	-1.03	-0.51
R_{vdW}-S_8 (%)	65.72	40.04	79.06	67.01	72.87
E_{ad}^{vdW}-Li_2S_8 (eV)	-4.99	-5.44	-3.61	-8.54	-9.89
E_{ad}^{no-vdW}-Li_2S_8 (eV)	-3.07	-3.80	-1.87	-5.85	-7.78
R_{vdW}-Li_2S_8 (%)	38.52	30.28	48.34	31.57	21.29
E_{ad}^{vdW}-Li_2S_6 (eV)	-4.40	-4.54	-3.24	-7.67	-5.48
E_{ad}^{no-vdW}-Li_2S_6 (eV)	-2.86	-3.37	-1.76	-5.50	-3.92
R_{vdW}-Li_2S_6 (%)	35.06	25.88	45.72	28.37	28.49
E_{ad}^{vdW}-Li_2S_4 (eV)	-4.18	-5.20	-3.51	-7.42	-5.62
E_{ad}^{no-vdW}-Li_2S_4 (eV)	-3.05	-4.13	-2.44	-5.64	-4.51
R_{vdW}-Li_2S_4 (%)	27.02	20.49	30.52	23.95	19.75
E_{ad}^{vdW}-Li_2S_2 (eV)	-4.58	-5.67	-4.02	-7.26	-9.63
E_{ad}^{no-vdW}-Li_2S_2 (eV)	-3.77	-4.89	-3.22	-5.91	-8.76
R_{vdW}-Li_2S_2 (%)	17.73	13.84	19.94	18.69	9.00
E_{ad}^{vdW}-Li_2S (eV)	-4.65	-5.79	-4.48	-6.87	-8.06
E_{ad}^{no-vdW}-Li_2S	-4.02	-5.15	-3.87	-5.65	-7.09

(eV)					
R_{vdW}-Li_2S (%)	13.67	10.97	13.71	17.74	12.03

Table S4. Calculated values of E_{DFT} and G^{corr} based on the adsorption configurations of S_8/Li_2S_n (n = 1, 2, 4, 6, and 8) on LaBO$_3$ (B = Cr, Mn, Fe, Co, and Ni) surfaces.

	$LaCrO_3$	$LaMnO_3$	$LaFeO_3$	$LaCoO_3$	$LaNiO_3$
E_{DFT}-S_8 (eV)	-771.47	-749.11	-716.20	-661.25	-628.39
G^{corr}-S_8 (eV)	0.01	0.00	0.00	0.02	-0.02
E_{DFT}-Li_2S_8 (eV)	-780.39	-757.70	-724.47	-672.73	-642.47
G^{corr}-Li_2S_8 (eV)	0.08	-0.01	0.04	0.12	0.15
E_{DFT}-Li_2S_6 (eV)	-771.69	-748.70	-716.00	-663.77	-629.96
G^{corr}-Li_2S_6 (eV)	0.06	0.00	0.00	0.10	-0.02
E_{DFT}-Li_2S_4 (eV)	-762.95	-740.83	-707.75	-654.99	-621.58
G^{corr}-Li_2S_4 (eV)	0.06	0.05	0.05	0.09	0.06
E_{DFT}-Li_2S_2 (eV)	-754.06	-732.02	-698.97	-645.55	-616.30
G^{corr}-Li_2S_2 (eV)	0.08	0.05	0.06	0.13	0.14
E_{DFT}-Li_2S (eV)	-749.02	-727.02	-694.31	-640.04	-609.62
G^{corr}-Li_2S (eV)	0.11	0.02	0.06	0.07	0.11

Table 5. Parameter calculations for LaBO$_3$ (B = Cr, Mn, Fe, and Co) electrocatalysts during the adsorption of Li_2S molecule.

	$LaMnO_3$−Li_2S	$LaCrO_3$−Li_2S	$LaFeO_3$−Li_2S	$LaCoO_3$−Li_2S
Δq−O (e)	-0.24	-0.25	-0.53	-0.84
Δq−B-site (e)	-0.53	-0.39	-0.16	-0.12
Decomposition energy barriers of Li_2S (eV)	2.38	2.03	1.98	1.67

References

1. V. Wang, N. Xu, J.-C. Liu, G. Tang and W.-T. Geng, *Comput. Phys. Commun.*, 2021, **267**, 108033.
2. P. Sujatha Devi and M. Subba Rao, *J. Solid State Chem.*, 1992, **98**, 237-244.
3. M. A. Señarís-Rodríguez and J. B. Goodenough, *J. Solid State Chem.*, 1995, **116**, 224-231.
4. H. Falcón, A. E. Goeta, G. Punte and R. E. Carbonio, *J. Solid State Chem.*, 1997, **133**, 379-385.
5. P. M. Raccah and J. B. Goodenough, *Physical Review*, 1967, **155**, 932-943.